Journal of Taibah University Medical Sciences (2023) 18(5), 1018–1029

Taibah University

Journal of Taibah University Medical Sciences

www.sciencedirect.com

Original Article

Pharmacokinetic profiling of quinazoline-4(3H)-one analogs as EGFR inhibitors: 3D-QSAR modeling, molecular docking studies and the design of therapeutic agents

Sagiru Hamza Abdullahi, PhD *, Adamu Uzairu, PhD, Gideon Adamu Shallangwa, PhD, Sani Uba, PhD and Abdullahi Bello Umar, PhD

Department of Chemistry, Faculty of Physical Sciences, Ahmadu Bello University, Zaria, Kaduna State, Nigeria

Received 8 October 2022; revised 13 December 2022; accepted 27 February 2023; Available online 9 March 2023

المخلص

أهداف البحث: تصنف أورام الثدي على أنها أكثر أنواع الأورام التي تم تحديدها بين النساء على مستوى العالم مع أكثر من 1.7 مليون حالة سنويا، تمثل 11.9٪ من إجمالي حالات السرطان. أظهرت الأدوية المضادة لأورام الثدي المعتمدة العديد من الآثار الجانبية ويطور بعض المرضى مقاومة في مرحلة العلاج المبكرة. هدفت هذه الدراسة إلى استخدام نهج إن-سيليكو لتحديد وتصميم العوامل العلاجية المحتملة.

طرق البحث: تم تطوير نماذج قوية ثلاثية الأبعاد للعلاقات بين البنية والنشاط الكمي باستخدام كينازولين -4 (3 هـ) - نظائرها كمثبطات لمستقبلات عامل نمو البشرة. تم اختيار أفضل نموذج بناءً على معايير إحصائية، وتم استخدامه لاحقًا في تصميم عوامل علاجية أكثر فاعلية. تم تنفيذ محاكاة الالتحام الجزيئي باستخدام مجموعة البيانات والمركبات المصممة لتحديد مركبات الرصاص التي تم فحصها بشكل أكبر عبر التنميط الدوائي بمساعدة موقعي الإنترنت سويس-أدمي وبيكي-سيسأم.

النتائج: اجتازت عمليات التحقق الداخلية لأفضل تحليل للمجال الجزيئي المقارن ونماذج تحليل مؤشرات التشابه الجزيئي المقارنة (ر 2 = 0.855 و0.895) و (كيو 2 = 0.570 و0.599) قيم العتبة للاعتراف بنموذج علاقات النشاط الكمي المتسق. تم التحقق من صحة النماذج المبنية خارجيًا باستخدام ستة مركبات كمجموعة اختبار، وكشف عن معامل الارتباط المتوقع المرضي (ر 2 = 0.657 و 0.681). تعرض نموذج تحليل مؤشرات التشابه الجزيئي المقارن مع أفضل المعلمات الإحصائية لمزيد من التحقق من مجال التطبيق وتم اكتشاف ثلاث مؤثرات فقط من مجموعة الاختبار، ثم تم استخدامه لتصميم خمس مركبات جديدة بأنشطة تتراوح من 5.62 إلى 6.03. أكدت دراسات الالتحام الجزيئي للمركبات 20 إلى 26 بدرجات تراوحت من -163.729 إلى -169.796 كمركبات رصاص، مع درجات أعلى في الالتحام مقارنة بمركب جيفيتينيب (-127.495). أيضا، تظهر المركبات المصممة درجات رسو أفضل تتراوح من -171.379 إلى -179.138.

الاستنتاجات: أكدت الدراسات الدوائية المركبات 20 ، 24 ، 26 والمركبات المصممة 2 ، 3 ، 5 كأدوية مرشحة مجدية. ومع ذلك، يمكن التحقق من صحة النتائج النظرية تجريبيا.

الكلمات المفتاحية: سرطان الثدي؛ قاعدة ليبينسكي؛ الالتحام الجزيئي؛ كينازولين؛ العلاقات الكمية ثلاثية الأبعاد الهيكلية والنشاط

Abstract

Objectives: Breast tumor is ranked as the most common tumor type identified among women globally with over 1.7 million cases annually, representing 11.9% of the total number of cancer cases. Approved anti-breast tumor drugs exhibit several side effects and some patients develop resistance during the early treatment stage. This study aimed to use an in-silico approach to identify and design potential therapeutic agents.

Methods: Robust 3D-QSAR models were developed using quinazoline-4(3H)-one analogs as EGFR inhibitors. The best model was then selected based on statistical parameters and was subsequently used to design more potent therapeutic agents. Molecular docking simulation was executed using the data set and the designed compounds to identify lead compounds which were further screened by pharmacokinetic profiling by applying SwissADME and pkCSM software.

* Corresponding address: Department of Chemistry, Faculty of Physical Sciences, Ahmadu Bello University, P.M.B.1045, Zaria, Kaduna State, Nigeria.

E-mail: sagirwasai@gmail.com (S.H. Abdullahi)

Peer review under responsibility of Taibah University.

ELSEVIER Production and hosting by Elsevier

 https://doi.org/10.1016/j.jtumed.2023.02.015

Results: Internal validations of the best CoMFA and CoMSIA models ($R^2 = 0.855$ and 0.895; $Q^2 = 0.570$ and 0.599) passed the threshold values for the establishment of a consistent QSAR model. The constructed models were further validated externally using six compounds as a test set, thus revealing a satisfactory predicted correlation coefficient ($R^2_{pred} = 0.657$ and 0.681). The CoMSIA_SHE models with the best statistical parameters were further subjected to applicability domain checks and only three influentials were detected. These were then utilized to design five novel compounds with activities ranging from 5.62 to 6.03. Molecular docking studies confirmed that compounds 20 to 26, with docking scores ranging from −163.729 to −169.796, represented lead compounds with higher docking scores compared to Gefitinib (−127.495). Furthermore, the designed compounds exhibited better docking scores ranging from −171.379 to −179.138.

Conclusions: Pharmacological studies identified compounds 20, 24 26 and the designed compounds 2, 3, 5 as feasible drug candidates. However, these theoretical findings should now be validated experimentally.

Keywords: 3D-QSAR; ADMET; Breast cancer; Lipinski's rule; Molecular docking; Quinazolin-4(3H)-one

Introduction

Breast tumor is ranked as the most common form of tumor identified among women globally with over 1.7 million cases, representing 11.9% of the overall number of cancer cases.[1,2] Epidermal growth factor receptor (EGFR) plays an essential role in the regulation of cell evolution and is deemed to be the most commonly investigated tyrosine kinase (TK) target. The EGFR plays a pivotal role in cell dispersal and metastasis.[3] Furthermore, unrestrained activation through point mutation and other processes has resulted in a significant number of clinical cancer cases.[4] Over recent years, instantaneous diagnosis, revision of the mechanisms and pathways of breast cancer (BC). Continuous advances in treatment have played a crucial part in abating the associated fatality rate. Chemotherapy remains the principal strategic therapy as this can annihilate cancer cells quicker; however, antagonistic side effects and increasing resistance during the early treatment stage, represents significant limitations of approved drugs. Therefore, the design of improved and safer drugs is urgently required.[5,6] In-silico aided drug-design techniques were recently engaged in enhancing, accelerating and simplifying the drug discovery process.[7] 3-Dimensional Quantitative Structure Activity Relationship (3D-QSAR) is one of the modern in-silico techniques used in the design of novel drugs in which the three-dimensional (3D) structural features of molecules are correlated with biological activity. Significant components of 3D-QSAR include comparative molecular field analysis (CoMFA) and comparative molecular similarity indices analysis (CoMSIA). Steric and electrostatic fields are interrelated with bioactivity in CoMFA modeling, while in CoMSIA modeling, hydrophobic, hydrogen bond donors/acceptors, and steric/electrostatic fields, are interrelated with bioactivity.[8,9] Even though the CoMSIA model is an advanced version of the CoMFA model, the latter is still an efficient approach in the prediction of activity during drug design. As such, in this research, different combinations of the two models were developed using quinazolin-4(3H)-ones analogs as EGFR inhibitors and key statistical variables were analyzed to identify the best model which was then used to design more potent inhibitors. Molecular docking and pharmacokinetic analysis were performed to study the mode of interactions of selected molecules with the target receptor and to ascertain their drug-likeliness status.

Materials and Methods

Data set collection and energy minimization

Thirty six quinazoline-4(3H)-ones series were retrieved from the literature.[6,10] Two-dimensional (2D) structures were created *via* PerkinElmer ChemDraw software and then transformed to a 3D format with Spartan v14.0 software. This information was then used to analyze energy minimization *via* density functional theory (DFT) calculations with a B3LYP/6-31G* basis set.[11] Structures of the quinazoline-4(3H)-ones are presented in Supplementary Table 1.

Ligand alignment

The most crucial step in 3D-QSAR modeling is ligand alignment. In this study, compounds were allied on the quinazolin-4-one scaffold using the distill rigid module in SYBYL-X 2.1.1 software with compound 20 as the template.

Data set division

The aligned molecules were divided into thirty training and six test sets with the random selection approach in SYBYL-X 2.1.1 software. The inhibitive activities (IC_{50}) of compounds were changed to a logarithmic scale (pIC_{50}) using equation (1) to minimize data skewness. The modeling set was then subjected to model building while the test set was used for external validation.

$$pIC_{50} = -\log_{10}(IC_{50} \times 10^{-6}) \quad (1)$$

CoMFA and CoMSIA modeling

In CoMFA modeling, the allied compounds were taken in a 3D cubic frame produced spontaneously with a 2.0 Å grid layout. Tripos force field with a SP^3 C^+ probing atom of 1.52 Å Van Der Waals radius was used to create steric (Lennard-Jones 6−12 potential) and electrostatic (Coulombic potential) fields with a distance dependent dielectric at each lattice point. To reduce noise and increase

field computation, the column filtering value was set to a default parameter (2.0 kcal/mol). In CoMSIA modeling, steric (S), electrostatic (E), hydrophobic (H), hydrogen bond donor (D), and acceptor (A), fields were computed with a sp^3 C^+ of radius 1.0 Å and by setting the attenuation factor to a default 0.3.[11,12] The partial least square approach (PLS) was used in a cross-validation study by adopting force field descriptors as the input variables and bioactivities as the output variables for modeling studies.[13,14]

Molecular docking studies

EGFR x-ray crystallized structures were retrieved from a protein data bank (pdb id: 2ITO) and prepared on the Molegro virtual docker (MVD) work space by eliminating solvent molecules and the co-crystallized ligand. Amino acid residues with faulty structures were restored and restructured. Then, the docking process was run for more than 50 rounds and 5 poses on the MVD workspace. MolDock score GRID was adopted as the scoring functions for the best poses determined and the complexes were analyzed and interpreted using Discovery Studio 3.5[11].

Pharmacokinetic studies

The medicinal properties of each compound were predicted by pkCSM and SwissADME online web servers.[15–17]

Results and discussion

Ligand alignment

Molecules were aligned based on the quinazolin-4-one common core (Figure 1) using the distill rigid method with compound 20 as the template (Figure 2).

3D-QSAR modeling

During CoMFA modeling, electrostatic and steric field contributions were used as input variables while the training set pIC_{50} was opted as the output variable. PLS regression was utilized for modeling and the assessment parameters of the best model (CoMFA_S) were $R^2 = 0.872$ with three latent components, $Q^2 = 0.597$, and a standard error of 0.154. The results of statistical validation from all possible CoMFA models are shown in Supplementary Table 2. With regards to CoMSIA modeling, the assessment parameters of the probable models obtained from the permutation of steric (S), electrostatic (E), hydrophobic (H), hydrogen bond donor (D), and acceptor (A) fields, are also presented in Supplementary Table 2. Nevertheless, the CoMSIA_SHE model exhibited the best Q^2 and R^2 values of 0.666 and 0.982 with nine latent components, and a standard error of 0.0655765. To further ascertain the statistical relevance of the CoMSIA_SHE model, we subjected this model to applicability domain (AD) studies which enabled the discovery of influential and structural outliers graphically using a William's plot (Figure 3), a plot of the standardized residuals of compounds against leverage values. The cut-off leverage (h*) calculated using equation (2), was found to be 0.4 and the compounds were within the defined AD space except for compounds 17, 21, and 28 from the test which were considered as influentials (i.e., $h > h^*$). Outliers were not detected as the standardized residuals of the compounds were within the ±3 region.[11] These assessment parameters showed that the best models exhibited dependable predictive capacity (Table 1); hence, these were used to compute the pIC_{50} values of the data set (Table 2). The experimental activities of the compounds correlated with their predicted values, as revealed by Supplementary Figures 1 and 2.

$$h^* = 3(D + 1)/N \quad (2)$$

In equation (2), D represents the SHE descriptors while N is the number of training set samples.

Contour map analysis

The contours of 3D-QSAR models provide crucial information that can be used to explore essential areas in the 3-dimensional space around a molecule where field modification considerably affects the biological activity. Compound 20 (Figure 4) was used to generate and view contour maps.

CoMFA_S contour map

The CoMFA_S contour map is shown in Figure 5 and is represented by green and yellow contours. The green contour recommends that the introduction of bulky groups around a region helps to increase bioactivity while the yellow contour implies that bulky groups around a region lead to a reduction

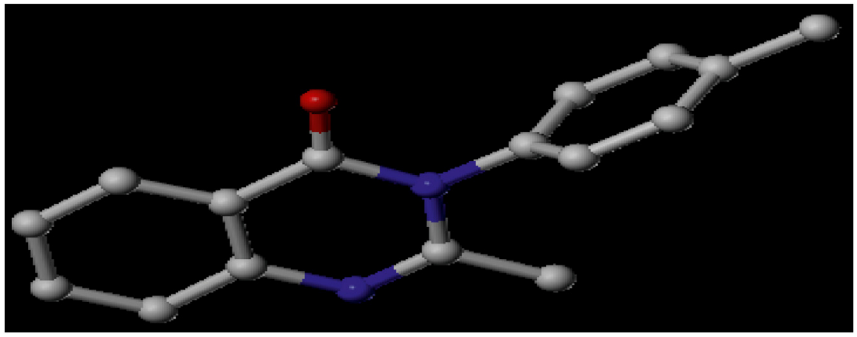

Figure 1: Three-dimensional structure of the quinazoline-4-one common core.

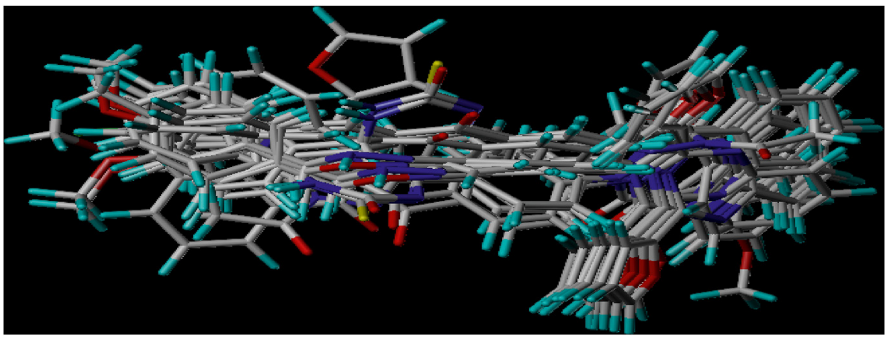

Figure 2: Three-dimensional representation of the aligned compounds.

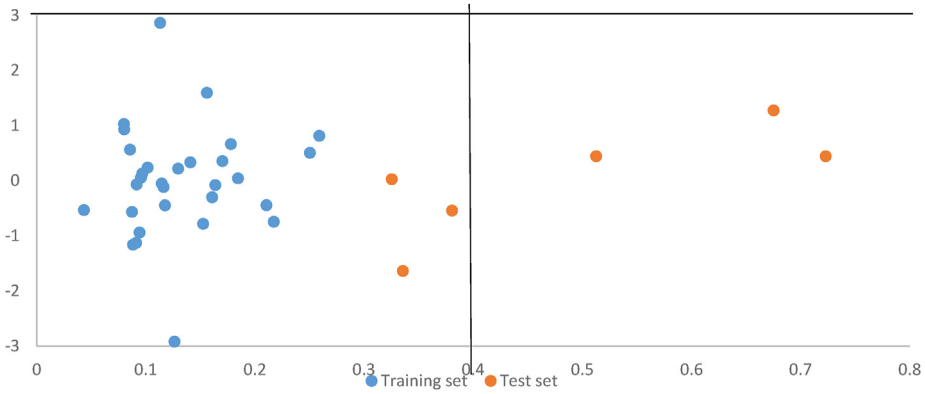

Figure 3: William's plot of the CoMSIA_SHE model.

Table 1: Assessment parameters of the best 3D-QSAR models.

Model	Q^2	R^2	F	R^2_{test}	Field fractions				
					S	E	H	A	D
CoMFA/S	0.597	0.872	65.808	0.6646	1	–	–	–	–
CoMSIA/SHE	0.666	0.982	53.174	0.6975	0.445	0.350	0.195	–	–

in the bioactivity of molecules.[18] Green contours were detected around the p-chlorophenyl group, close to the 8-position of the quinazoline-4-one scaffold and the benzene thiazolidinone group. This might be the reason for the higher activity of compound 29 ($pIC_{50} = 4.65$) which has a bulky Br group at position 8 of the quinazoline-4-one when compared to compound 30 ($pIC_{50} = 4.30$). The yellow contours are located close to the 6, 7 positions, around the carbonyl group, and close to the thiazolidinone group sulfur atom.

CoMFA_E contour map

The contour map for CoMFA_E is shown in Figure 6 and represented by blue and red contours. Blue contours present areas where electron negative groups improve activity while the red contour illustrates the region in which electron negative groups reduce the bioactivity of the compound. A large blue contour was detected near the 6,8-positions, and C═O group of the quinazoline scaffold, at the ortho positions of the p-chloro phenyl group, and close to the Benzamide group. Furthermore, red contours were found to be situated close to the pyrimidinone group, and at the ortho position of the phenyl group attached to the thiazolidinone group. This might be the reason why compounds 16 to 29, with electronegative bromine at the 6,8-positions of the quinazoline group, have higher activities than compounds 29 to 36.

CoMSIA contour map

Next, steric, hydrophobic, and electrostatic fields were investigated in the In the CoMSIA_SHE contour map. The CoMSIA_S contour is analogous to the CoMFA_S model; therefore, this evaluation focused on hydrophobic and electrostatic contours. In the hydrophobic contour map, the yellow contour illustrates the regions where an increase in hydrophobicity will improve the activity of a compound while the white contour illustrates undesirable

Table 2: Predicted activities obtained from the best 3D-QSAR models.

Name	CoMFA_S			CoMSIA_SHE		
	Exp pIC_{50}	Pred pIC_{50}	Residue	Pred pIC_{50}	Residue	MolDock score
1	4.37	4.36	0.01	4.36	0.01	−133.83
2[a]	3.90	4.12	−0.22	4.17	−0.27	−137.89
3	3.95	4.09	−0.15	3.95	−0.00	−135.44
4	4.8	4.88	−0.08	4.78	0.02	−136.90
5	5.18	4.99	0.18	5.15	0.03	−133.31
6	4.25	4.99	−0.75	4.25	−0.00	−134.18
7	4.36	4.14	0.22	4.38	−0.02	−137.60
8	4.53	4.46	0.07	4.56	−0.03	−146.93
9	4.51	4.52	−0.01	4.51	0.00	−143.75
10	3.93	4.21	−0.28	3.89	0.04	−129.35
11	3.94	4.11	−0.17	3.93	0.01	−130.38
12	4.60	4.55	0.05	4.64	−0.04	−129.99
13	4.80	4.84	−0.04	4.76	0.04	−145.63
14	4.52	4.50	0.02	4.55	−0.03	−131.50
15[a]	4.2	4.87	−0.67	4.32	−0.12	−153.69
16	4.95	5.15	−0.20	4.96	−0.01	−141.71
17[a]	4.79	5.18	−0.39	4.80	−0.01	−145.52
18	5.22	5.19	0.02	5.20	0.02	−148.92
19	5.04	5.08	−0.04	5.10	−0.06	−147.23
20	5.52	5.24	0.28	5.01	0.51	**−168.49**
21[a]	4.92	4.91	0.01	4.71	0.21	**−163.73**
22	4.92	4.85	0.07	4.94	−0.02	**−169.71**
23	4.63	4.87	−0.24	4.62	0.01	**−165.85**
24	4.85	4.74	0.11	4.89	−0.04	**−169.79**
25	5.04	4.82	0.22	4.95	0.09	**−163.80**
26	4.95	5.19	−0.25	5.11	−0.16	**−168.36**
27	4.74	4.76	−0.02	4.76	−0.02	−159.33
28[a]	4.63	4.71	−0.08	4.64	−0.01	−119.44
29	4.65	4.69	−0.04	4.62	0.03	−124.58
30	4.30	4.25	0.05	4.35	−0.05	−120.30
31	4.30	4.15	0.15	4.25	0.05	−118.18
32	4.00	4.15	−0.15	3.94	0.06	−115.13
33	4.30	4.37	−0.07	4.30	0.00	−113.97
34	4.30	4.14	0.16	4.36	−0.06	−121.61
35[a]	4.00	4.43	−0.43	4.56	−0.56	−120.24
36	4.30	4.22	0.08	4.29	0.01	−128.89
Gefitinib						−127.49

Bold values signifies predicted activities obtained from the CoMFA_S and CoMSIA_SHE models.
[a] Test set.

regions for the introduction of hydrophobic groups. Yellow contours were observed near the nitrogen atom of the quinazoline-4-one scaffold and close to the ortho position of the phenyl group attached to the thiazolidinone group. A large white contour was located close to the 6,8-dibromo groups attached to the quinazoline-4-one scaffold. A CoMSIA_H contour map for compound 20 is presented in Figure 7.

In the CoMSIA_E map (Figure 8), blue contours were detected close to positions 4−6 and the C═O group of the quinazoline-4-one scaffold; another blue contour was located close to the sulfur atom. Red contours were observed around the 2, 3-positions of the quinazoline scaffold and close to the thiazolidinone C═O group. The CoMSIA_E model formed fewer contours when compared to the corresponding CoMFA_E model. This might be attributed to the fact that Lennard-Jones 6−12 and coulombic potentials were used in generating the CoMFA descriptors while Gaussian potentials were used in CoMSIA modeling.[8]

The design of new EGFR inhibitors

Based on the CoMSIA_SHE model contour maps, five novel compounds were designed using Figure 9 as a template. The designed compounds were aligned on the quinazoline-4-one common core in a similar manner using the distill rigid approach; their activities were predicted using the CoMSIA_SHE model. These compounds exhibited better EGFR inhibitive activities, ranging from 5.62 to 6.03.

Molecular docking studies

Before beginning the docking process, Gefitinib was redocked with the initial EGFR active pocket and the initial and redocked poses were superimposed using Discovery Studio software, as shown in Figure 10. The RMSD value was found to be 1.35 Å, thus confirming the reliability of the docking algorithm utilized in this research.[21] As shown

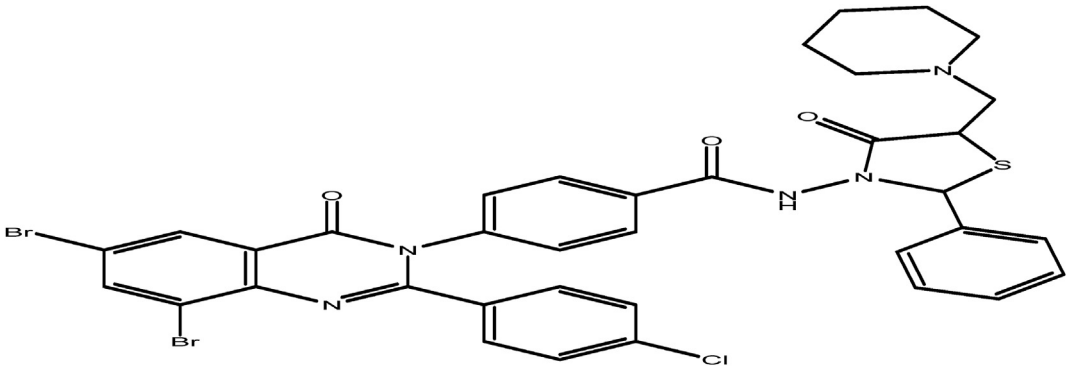

Figure 4: Structure of compound 20.

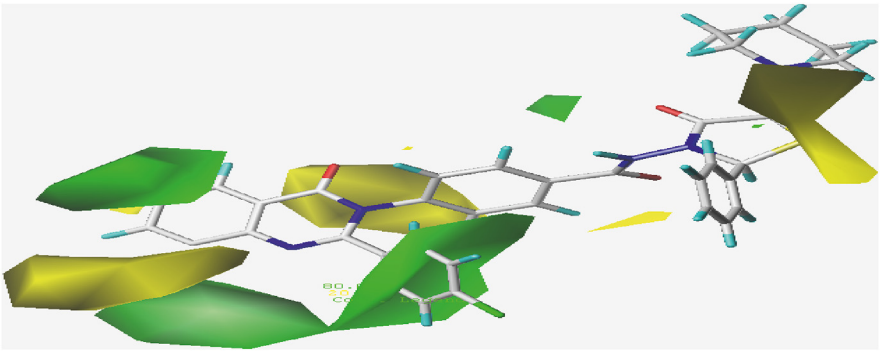

Figure 5: CoMFA_S contour map.

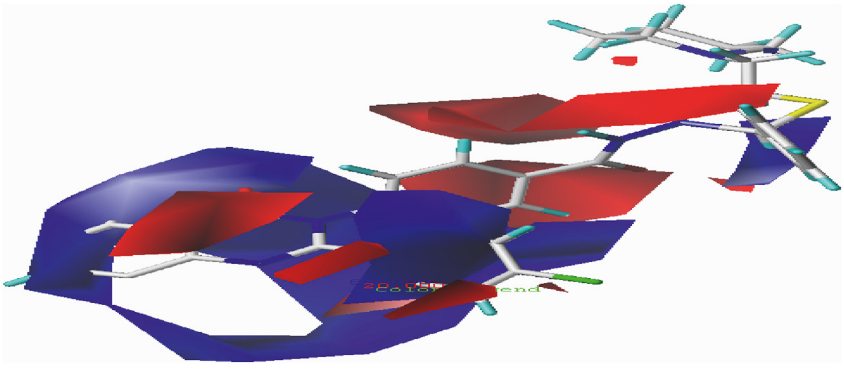

Figure 6: CoMFA_E contour map.

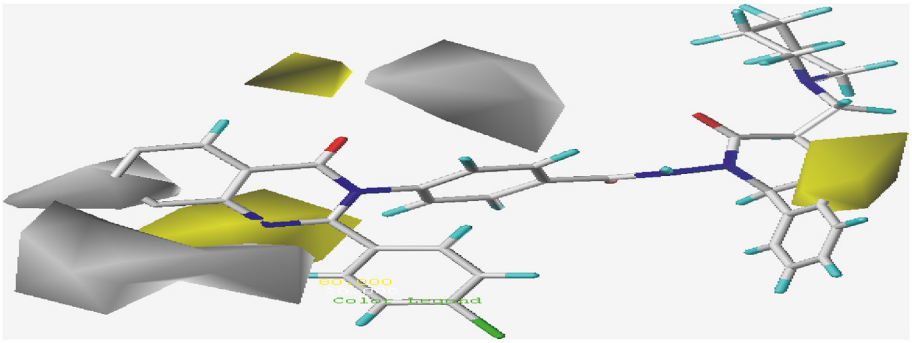

Figure 7: CoMSIA_H contour map.

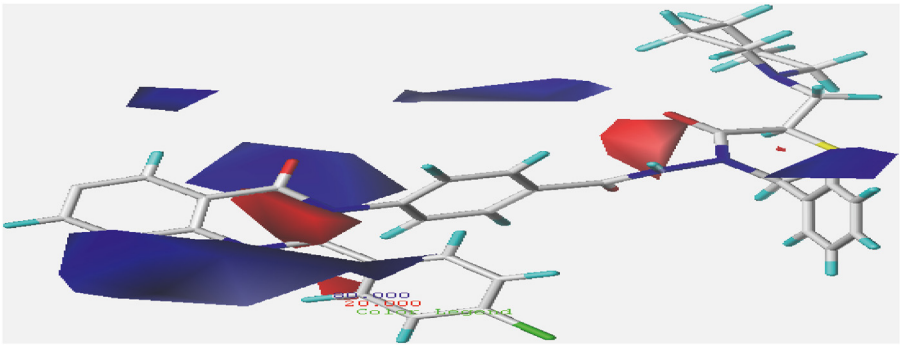

Figure 8: CoMSIA_E contour map.

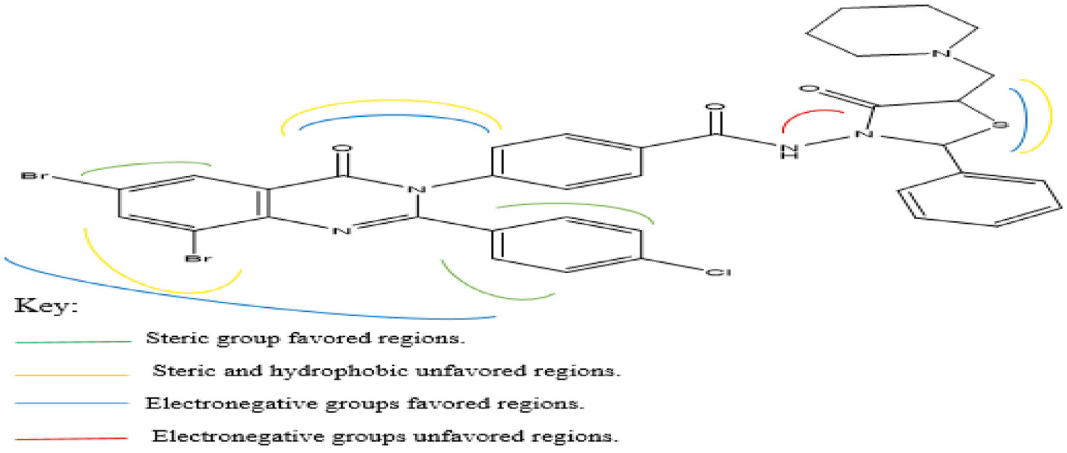

Figure 9: Structure-activity relationship derived from the CoMSIA_SHE model.

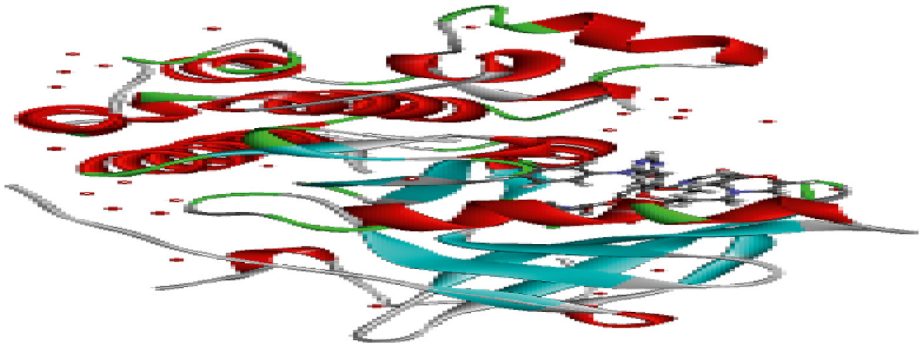

Figure 10: Three-dimensional structure of the superimposed poses of Gefitinib.

in Table 2, the binding affinities of the compounds ranged from −113.97 to −169.796. Compounds 20 to 26 exhibited the highest MolDock scores, ranging from −163.729 to −169.796, when compared to the other compounds and Gefitinib (−127.495); therefore, these were selected as lead compounds. Their interactions with the EGFR active site are shown in Supplemental Table 2, and the interactions of compounds 24, 22, and 20 with the best docking scores are presented.

EGFR/24 complex interactions involved the quinazoline-4-one C═O group forming a conventional hydrogen bond with SER719 at 2.06 Å, the thiazolidin-4-one group hydrogen atom forming carbon−hydrogen bond with GLU762 at 2.35 Å, LYS745 forming double π-cation interactions, and ASP855 forming a π-anion electrostatic interactions. In addition, LEU747, ALA755, MET766, ALA743, VAL726, LEU718, and LEU792 formed hydrophobic interactions. The 2D interactions of the EGFR/24 complex are presented in Figure 11.

EGFR/22 complex interactions included Thiazolidin-4-one C═O and the NH hydrogen atom forming two conventional hydrogen bonds with ASN842 and ASP855 at

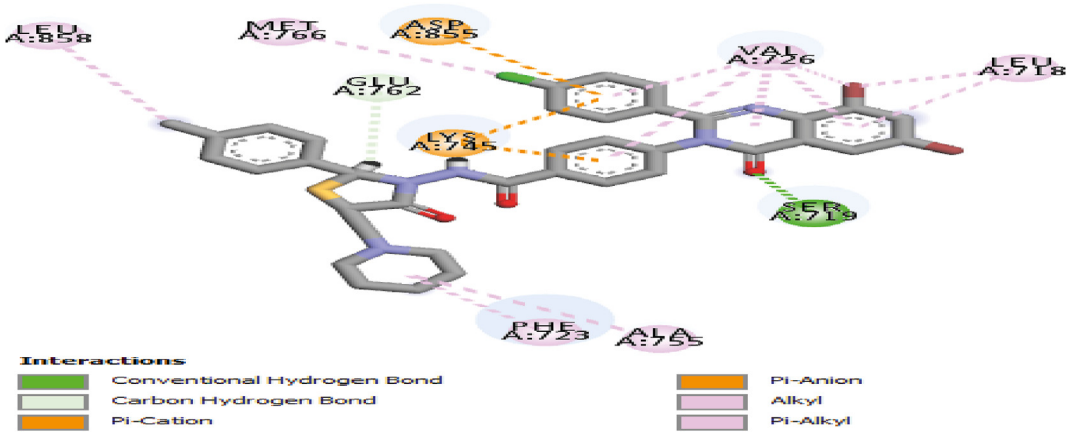

Figure 11: Two-dimensional interactions of the EGFR/24 complex.

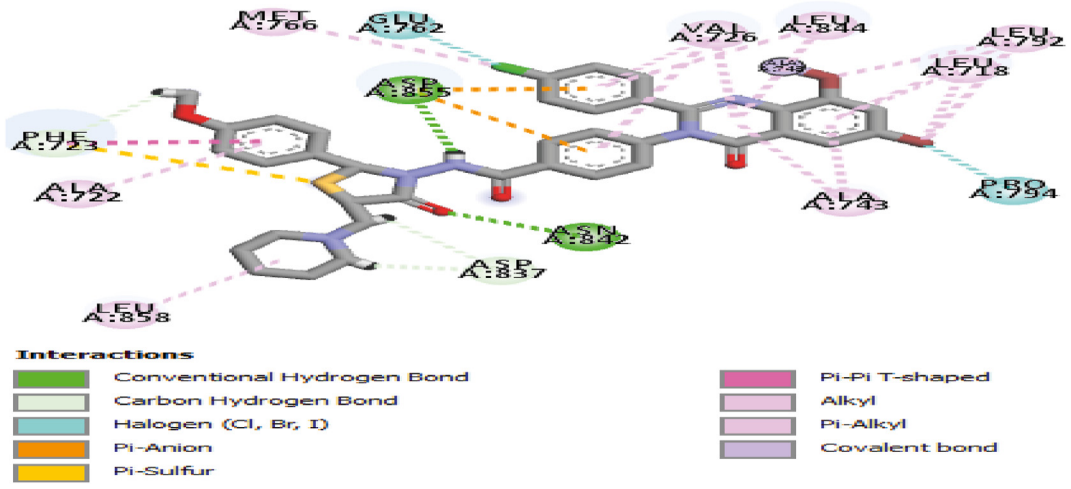

Figure 12: Two-dimensional interactions of the EGFR/22 complex.

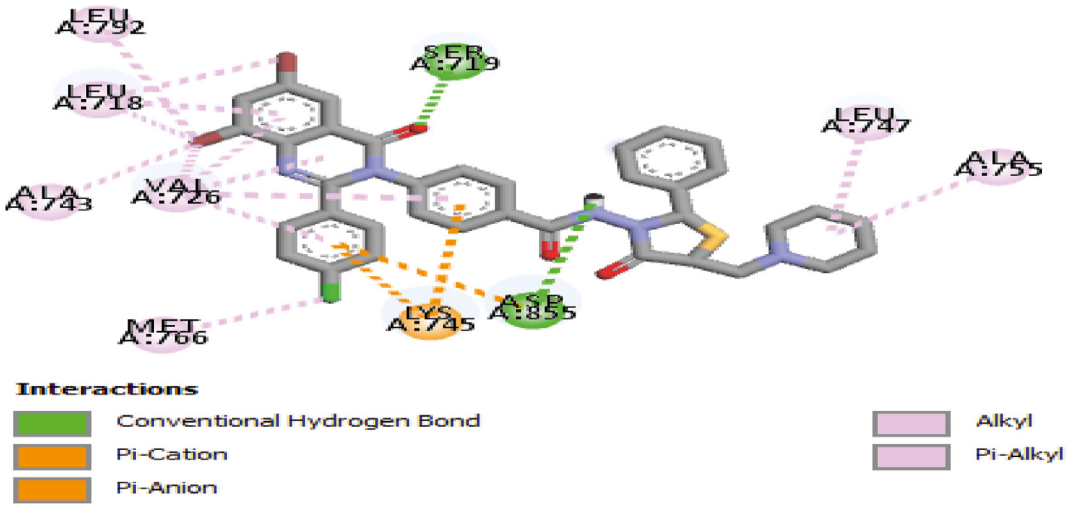

Figure 13: Two-dimensional interactions of the EGFR/20 complex.

Table 3: Structure-predicted pIC_{50} and docking scores of the designed compounds.

S/No	Structure	Predicted pIC_{50}	Docking score
1	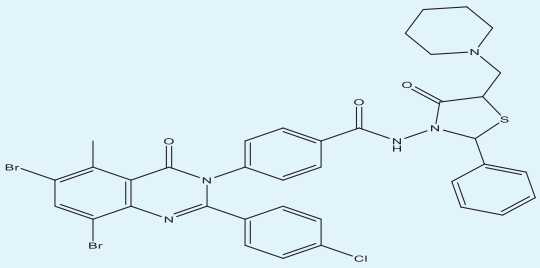	5.82	−174.43
2	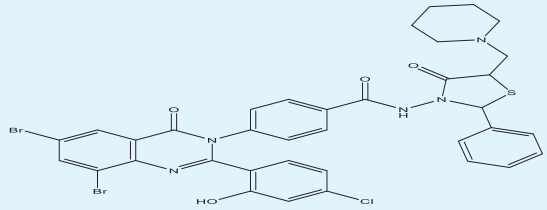	5.67	−173.568
3	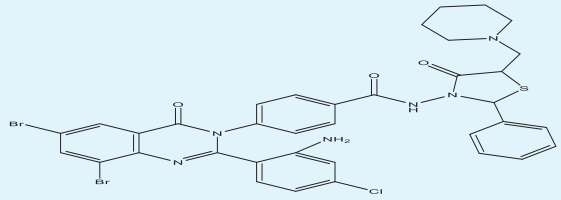	6.03	−179.138
4	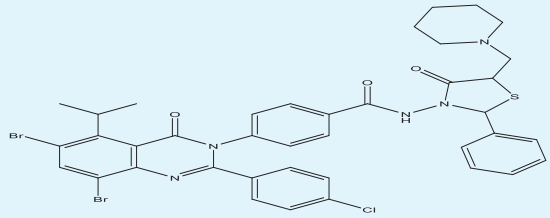	5.62	−171.379
5	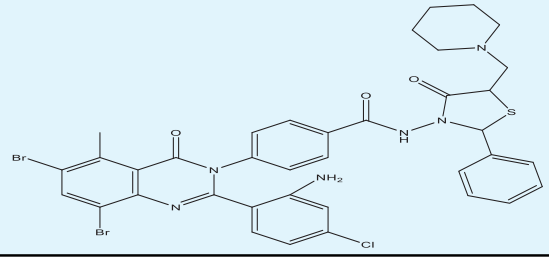	5.71	−174.622

2.89 Å and 2.82 Å. ASP837 and PHE723 formed three carbon−hydrogen bonds with CH_2 and OCH_3 groups at 2.32, 2.68 Å, and 2.88 Å. GLU762 and PRO794 formed two halogen interactions with chlorine and bromine atoms. ASP855 formed two π-anion interactions and PHE723 formed Pi−Pi T-shaped interactions while LEU858, ALA722, MET766, VAL726, LEU844, LEU792, LEU718, ALA743 formed hydrophobic interactions. The 2D interactions of the EGFR/22 complex are shown in Figure 12.

EGFR/20 complex interactions included the quinazoline-4-one C═O group and NH hydrogen atom forming two conventional hydrogen bonds with SER719 and ASP855 at 2.15 Å and 2.45 Å. LYS745 forming two π-cations while ASP855 formed other π-anion interactions. LEU747, ALA755, MET766, ALA743, VAL726, LEU718, and LEU792 formed hydrophobic interactions. 2D interactions of the EGFR/20 complex are presented in Figure 13.

Molecular docking studies of the designed compounds

The designed compounds were optimized and docked with the EGFR binding site to study the nature of interactions with residues in the active; results are presented in Table 3. The compounds exhibited better binding affinities,

Table 4: Results of pharmacokinetic studies for the lead and designed compounds.

S/No	MW	TPSA	wLOGP	HBA	HBD	nLv	ABS	SA
Lead molecules								
20	807.98	112.84	3.92	5	1	1	0.55	5.34
21	809.95	122.07	5.76	6	1	2	0.17	5.26
22	838.01	122.07	6.93	6	1	2	0.17	5.47
23	839.98	131.30	5.77	7	1	2	0.17	5.40
24	822.01	112.84	4.23	5	1	1	0.55	5.47
25	823.98	122.07	6.07	6	1	2	0.17	5.38
26	823.98	133.07	4.62	6	2	1	0.55	5.41
Designed compounds								
1	822.01	112.84	5.23	5	1	2	0.17	5.49
2	823.98	133.07	4.62	6	2	1	0.55	5.40
3	823.00	138.86	4.51	5	2	1	0.55	5.46
4	850.06	112.84	6.04	5	1	2	0.17	5.76
5	837.02	138.86	4.82	5	2	1	0.55	5.60

ranging from −171.379 to −179.138, when compared to the lead compounds. Thus, they bound more effectively with EGFR binding sites and can be utilized as novel EGFR inhibitors targeting breast cancer.

Pharmacokinetic studies

Both the lead and the designed compounds were subjected to pharmacokinetic profiling with SwissADME software utilizing the Lipinski's rule of five which states that an orally administered drug must have molecular weight at most 500, a calculated logP no more than 5, fewer than 5 hydrogen bond donors, hydrogen bond acceptors lower than or equal to 10, and a topological polar surface area (TPSA) at most 140 $Å^2$. An entity that disputes at least two of these criteria may possess challenges related to bioavailability.[19] The findings of pharmacokinetic profiling (Table 4) illustrated that compounds 20, 24 and 26 and designed compounds 2, 3, and 5 violated only one of the rules (MW > 500); hence, these were considered to possess drug-likeness properties. The potentiality of the molecule to exhibit optimum permeability and bioavailability profile was assessed using bioavailability score (ABS) standards.[23] Compounds 20, 24 and 26, and designed compounds 2, 3, and 5, exhibited bioavailability scores of 0.55, thus demonstrating excellent oral bioavailability and agreement with Lipinski's rule. Synthetic accessibility (SA) assessment showed that these compounds can be easily synthesized as their respective scores were less than 10.

Evaluation of ADMET properties

To further confirm compounds 20, 24 and 26 and designed compounds 2, 3, and 5 as possible drug candidates, we next investigated ADMET properties. Essential parameters included intestinal (human) absorption, blood−brain-barrier (BBB) penetration, CYP450, and toxicities; these were predicted using the pkCSM online tool. The findings of the ADMET properties studies (Table 5) showed that the compounds have high intestinal (human) absorption ranging from 93.15 to 100%. Consequently, these compounds will be absorbed well by the human intestine because poorly absorbed molecules exhibit <30% HIA absorbance.[22] BBB and CNS grading were employed to establish the potentiality of molecules to permeate through the blood−brain barrier and central nervous system. A log BB > 0.3 suggested easy BBB permeability whereas a log BB < −1 suggests poor permeation properties. In addition, a log PS > −2 designates easy CNS permeation while a log PS < −3 suggests poor dispersal. The predicted logBB and log PS for the molecules suggested a non-BBB permeation status and good CNS permeability.[20] The body's physiological adjustment of a potential drug is mainly illustrated by its metabolism; therefore, drugs generally propose several metabolites which vary in pharmacological and physicochemical profiles. Cytochrome P450 (CYP450) plays an extensive role in molecular metabolism because this is the principal liver protein system responsible for oxidation (phase-1 metabolism). Most of the selected compounds are substrates and inhibitors of the most important class of super enzyme (CYP3A4) responsible for drug's metabolism. Results of toxicity studies revealed that the compounds do not possess AMES toxicity, thus conforming these as non-mutagenic; these are non-inhibitors of human ether a-go-go-related gene (hERG) cardiovascular toxicity and all exhibit positive hepatotoxicity

Table 5: ADMET properties of the selected drug candidates.

S/NO	Absorption	Distribution		Metabolism							Toxicity			
				Substrate			Inhibitors							
	HIA	BBB	CNS	2D6	3A4	1A2	2C19	2C9	2D6	3A4	AMES	hERGI inhibitor	Hepatotoxicity	Skin sensitization
Lead molecules														
20	93.496	−1.312	−1.547	No	Yes	No	Yes	Yes	No	Yes	No	No	Yes	No
24	93.15	−1.49	−1.579	No	Yes	No	No	Yes	No	Yes	No	No	Yes	No
26	100	−1.461	−1.726	No	Yes	No	Yes	Yes	No	Yes	No	No	Yes	No
Designed compounds														
2	100	−1.586	−1.735	No	Yes	No	No	Yes	No	No	No	No	Yes	No
3	100	−1.456	−1.456	No	Yes	No	No	Yes	No	No	No	No	Yes	No
5	100	−1.432	−1.642	No	Yes	No	Yes	Yes	No	Yes	No	No	Yes	No

potential with no skin sensitization. Based on pharmacokinetic profiling and ADMET properties, compounds 20, 24, and 26 and designed compounds 2, 3, and 5 can be adopted as potential drug candidates.

Conclusion

In this research, well validated CoMFA and CoMSIA 3D-QSAR models were developed using a series of 36 quinazolin-4(3H)-ones analogs as EGFR inhibitors. Statistical assessment of the developed models confirmed the CoMSIA_SHE model as the most robust with an R^2 of 0.895 and a Q^2 of 0.599 which exceeded the threshold values for generating a consistent QSAR model. William's plot of the model detected three influential compounds (17, 21, and 28) from the test set with leverage values greater than the threshold. Five novel derivatives, with activities ranging from 5.62 to 6.03 as predicted by the model, were designed using compound 20 as the template. Moreover, molecular docking studies confirmed that compounds 20–26 had the best docking scores when compared to Gefitinib as the lead compounds. Furthermore, the designed compounds exhibited higher docking scores when compared to the lead compounds. Evaluation of pharmacokinetic properties affirmed lead compounds 20, 24 and 26 and designed compounds 2, 3, and 5 as viable drug candidates that violated only one of the Lipinski's rule of five filter (MW $>$ 500) and displayed an excellent ADMET profile with no serious toxicity threat.

Recommendations

This study explores the applicability of in-silico techniques for the discovery of hypothetical drug candidates. Experimental synthesis of the lead compounds should now be carried out to validate our computational findings.

Source of funding

This research did not receive any specific grant from funding agencies in the public, commercial, or not-for-profit sectors.

Conflict of interest

The authors have no conflict of interest to declare.

Ethical approval

Not applicable.

Authors' contribution

SHA designed and executed the computational studies and drafted the manuscript, AU revised the manuscript, ABU analyzed the computational results, GAS and SU assessed the manuscript *via* Plagiarism checker as well as organizing the manuscript according to the journal format. All authors have critically reviewed and approved the final draft and are responsible for the content and similarity index of the manuscript.

Acknowledgment

Authors acknowledged all the members of theoretical chemistry research team for their guidance during the research and Ahmadu Bello University for providing the software and conducive atmosphere required for the research.

Appendix A. Supplementary data

Supplementary data to this article can be found online at https://doi.org/10.1016/j.jtumed.2023.02.015.

References

1. World Health Organization. *Global battle against cancer won't be won with treatment alone effective prevention measures urgently needed to prevent cancer crisis*. Lyon, London: International Agency for Research on Cancer; 2014.
2. Abdullahi SH, Uzairu A, Ibrahim MT, Umar. Chemo-informatics activity prediction, ligand based drug design, Molecular docking and pharmacokinetics studies of some series of 4, 6-diaryl-2-pyrimidinamine derivatives as anti-cancer agents. **Bull Natl Res Cent 2021**; 45: 167.
3. El-Azab AS, Al-Omar MA, Abdel-Aziz AAM, Abdel-Aziz NI, El-Sayed MAA, Aleisa AM, et al. Design, synthesis and biological evaluation of novel quinazoline derivatives as potential antitumor agents: molecular docking study. **Eur J Med Chem 2010**; 45: 4188–4198.
4. Tiwari SK, Sachan S, Mishra A, Tiwari S, Pandey V. The anticancer activity of some novel 4-anilino quinazoline derivatives as tyrosine kinase (EGFR) inhibitor and the quantitative structure activity relationships. **Int J Pharm Life Sci 2015**; 6: 4819–4828.
5. Kaplan W, World Health Organization, editors. **Priority medicines for Europe and the world: update**, 6–5; 2013.
6. Marwa F, Ahmed AB, Mahmoud Y. Design, synthesis, molecular modeling and anti-breast cancer activity of novel quinazolin-4-one derivatives linked to thiazolidinone, oxadiazole or pyrazole moieties. **Med Chem Res 2015**; 24: 2993–3007.
7. Ferreira R, Glaucius O, Andricopulo A. Integração das técnicas de triagem virtual e triagem biológica automatizada em alta escala: oportunidades e desafios em P&D de fármacos. **Quim Nova 2011**; 34(10): 1770–1778.
8. El-Mchichi L, El Aissouq A, Kasmi R, Belhassan A, El-Mernissi R, Ouammou A, et al. In silico design of novel pyrazole derivatives containing thiourea skeleton as anti-cancer agents using: 3D QSAR, drug-likeness studies, ADMET prediction and molecular docking. **Mater Today Proc 2021**. https://doi.org/10.1016/j.matpr.2021.03.152.
9. Chaube U, Chhatbar D, Bhatt H. Molecular dynamics simulations and molecular docking studies of benzoxazepine moiety as mTOR inhibitor for the treatment of lung cancer. **Bioorg Med Chem Lett 2016**; 26: 864–874.
10. Safoora P, Sedighe S, Ghadamali K, Marzieh R, Farshid H. Synthesis and cytotoxic evaluation of novel quinazolinone derivatives as potential anti-cancer agents. **Res Pharm Sci 2018**; 13(5): 450–459.
11. Sagiru HA, Uzairu A, Shallangwa GA, Uba S, Bello AU. In-silico activity prediction, structure based drug design, molecular docking and pharmacokinetic studies of selected quinazoline derivatives for their antiproliferative activity against triple negative breast cancer (MDA-MB231) cell line. **Bull Natl Res Cent 2022**: 1–23.

12. Richard D, Cramer DE, Patterson JD. Comparative molecular field analysis (CoMFA). 1. Effect of shape on binding of Steroids to carrier proteins. **J Am Chem Soc 1988**; 110(18): 5959–5967.
13. Wold S. Validation of QSAR's. **Quant Struct Act Relatsh 1991**; 10(3): 191–193.
14. Golbraikh A, Tropsha A. Beware of q2! **J Mol Graph Model 2002**; 20(4): 269–276.
15. Daina A, Michielin O, Zoete V. SwissADME: a free web tool to evaluate pharmacokinetics, drug-likeness and medicinal chemistry friendliness of small molecules. **Sci Rep 2016**; 20(4): 1–13.
16. Sagiru HA, Uzairu A, Shallangwa GA, Uba S, Bello AU. Molecular docking, ADMET and pharmacokinetic properties predictions of some di-aryl pyridinamine derivatives as estrogen receptor (Er +) kinase inhibitors. **Egypt J Basic Appl Sci 2022**; 9: 1 180–204.
17. Douglas E, Pires V, Tom L, David B. pkCSM: predicting small molecule pharmacokinetic and toxicity properties using graph-based signatures. **J Med Chem 2015**; 58(9): 4066–4072.
18. Gu X, Wang Y, Wang M, Wang J, Li N. Computational investigation of imidazopyridine analogs as protein kinase B (Akt1) allosteric inhibitors by using 3D-QSAR, molecular docking and molecular dynamic simulation. **J Biomol Struct Dyn 2021**; 39(1): 63–78.
19. Clark D. In Silico prediction of blood–brain barrier permeation. **Drug Discov Today 2003**; 8(20): 927–933.
20. Fabian U, Shallangwa GA, Uzairu A, Abdulkadir I. A combined 2D and 3D QSAR modeling, molecular docking study, design, and pharmacokinetic profiling of some arylimidamide-azole hybrids as superior L. donovani inhibitors. **Bul Natl Res Cent 2022**; 46(189): 1–24.
21. Sagiru HA, Uzairu A, Shallangwa GA, Uba S, Bello AU. Structure based design of some novel 3-methylquinoxaline derivatives through molecular docking and pharmacokinetics studies as novel VEGFR-2 inhibitors. **Chem Afr 2022**. https://doi.org/10.1007/s42250-022-00485-3.
22. Sagiru HA, Uzairu A, Shallangwa GA, Uba S, Bello AU. Computational modeling, ligand-based drug design, drug-likeness and ADMET properties studies of series of chromen-2-ones analogues as anti-cancer agents. **Bul Natl Res Cent 2022**; 46: 17.
23. Martin YC. A bioavailability score. **J Med Chem 2005**; 48(9): 3164–3170.

How to cite this article: Abdullahi SH, Uzairu A, Shallangwa GA, Uba S, Umar AB. Pharmacokinetic profiling of quinazoline-4(3H)-one analogs as EGFR inhibitors: 3D-QSAR modeling, molecular docking studies and the design of therapeutic agents. J Taibah Univ Med Sc 2023;18(5):1018–1029.